Developmental and Comparative Immunology 70 (2017) 69–79

Contents lists available at ScienceDirect

Developmental and Comparative Immunology

journal homepage: www.elsevier.com/locate/dci

Multiple major histocompatibility complex class I genes in Asian anurans: Ontogeny and phylogeny

Chelsea Didinger [a], John A. Eimes [a], Mette Lillie [b], Bruce Waldman [a, *]

[a] Laboratory of Behavioral and Population Ecology, School of Biological Sciences, Seoul National University, 1 Gwanak-ro, Gwanak-gu, Seoul 08826, South Korea

[b] Department of Medical Biochemistry and Microbiology (IMBIM), Genomics, Uppsala University, Box 582, 75123 Uppsala, Sweden

ARTICLE INFO

Article history:
Received 3 October 2016
Received in revised form
13 December 2016
Accepted 15 December 2016
Available online 25 December 2016

Keywords:
Anuran amphibians
Immunogenetics
Major histocompatibility complex
Non-model species
Supertypes

ABSTRACT

Amphibians, as the first terrestrial vertebrates, offer a window into early major histocompatibility complex (MHC) evolution. We characterized the MHC class I of two Korean amphibians, the Asiatic toad (*Bufo gargarizans*) and the Japanese tree frog (*Hyla japonica*). We found at least four transcribed MHC class I (MHC I) loci, the highest number confirmed in any anuran to date. Furthermore, we identified MHC I transcripts in terrestrial adults, and possibly in aquatic larvae, of both species. We conducted a phylogenetic analysis based on MHC I sequence data and found that *B. gargarizans* and *H. japonica* cluster together in the superfamily Nobleobatrachia. We further identified three supertypes shared by the two species. Our results reveal substantial variation in the number of MHC I loci in anurans and suggest that certain supertypes have particular physiochemical properties that may confer pathogen resistance.

1. Introduction

The vertebrate adaptive immune system discriminates self from non-self based on proteins encoded by the major histocompatibility complex (MHC) that bind peptides in specialized grooves (Klein, 1986). Together, MHC class I and II genes comprise the most highly polymorphic region of the vertebrate genome (Klein and Figueroa, 1986). The maintenance of this diversity is often attributed to parasite-driven balancing selection (Apanius et al., 1997; Bernatchez and Landry, 2003; Milinski, 2006; Piertney and Oliver, 2006), although sexual selection and inbreeding avoidance may play important roles (Edwards and Hedrick, 1998; Reusch et al., 2001).

Classical MHC class I (MHC IA) antigen binding sites are located in the alpha 1 and alpha 2 domains of the peptide binding region (PBR), encoded by exons 2 and 3 (Bjorkman et al., 1987; Hughes and Yeager, 1998; Saper et al., 1991). The number of transcribed MHC IA loci varies across vertebrate taxa. The most thoroughly studied amphibian, the African clawed frog *Xenopus laevis*, expresses only one MHC IA locus (Shum et al., 1993), but mammals can express up to three loci (Heimeier et al., 2009; Loker and Hofkin, 2015; Rammensee et al., 2013) and birds up to 16 loci (Bonneaud et al., 2006; Sepil et al., 2012).

As the first terrestrial vertebrates, amphibians may provide important insights into the understanding of MHC evolution. Until recently, knowledge of the amphibian MHC has been based on model species, *Xenopus* (Flajnik et al., 1986, 1991; Rollins-Smith et al., 1997) and *Ambystoma* (Fellah et al., 2002; Sammut et al., 1997, 1999; Tournefier et al., 1998). With the advent of new molecular methods, a broader understanding of MHC immunogenetics is emerging (Babik et al., 2008; Hauswaldt et al., 2007) and non-model species increasingly are being studied (Gong et al., 2013; Kiemnec-Tyburczy et al., 2012; Kosch et al., 2017; Lau et al., 2016; Lillie et al., 2014; Zhao et al., 2013; Zhu et al., 2014). For example, studies of MHC class I genes reveal widespread trans-species polymorphisms (Klein et al., 2007; Těšický and Vinkler, 2015). Selection, especially on the PBR of class I genes, has been demonstrated in many species (Kiemnec-Tyburczy et al., 2012; Lau et al., 2016; Zhao et al., 2013).

The complex life history of amphibians sets them apart from other vertebrates. During metamorphosis, many anurans transition from an aquatic to a terrestrial life form, undergoing radical reorganization of many tissue and organ systems including those involved in immune function (Robert and Ohta, 2009; Rollins-Smith, 1998). Class I is absent, or difficult to detect, on the surface

* Corresponding author.
E-mail address: waldman@snu.ac.kr (B. Waldman).

http://dx.doi.org/10.1016/j.dci.2016.12.003
0145-305X/

of tadpole cells but appears at metamorphic climax (Salter-Cid et al., 1998). The lack of class I expression in tadpoles may be a consequence of restricted numbers of lymphocytes or an adaptation to prevent autoimmunity from interfering with tissue reorganization (Flajnik et al., 1986; Flajnik and Du Pasquier, 1988; Rollins-Smith et al., 1997). Yet these results, based on the *Xenopus* model system, may not be widely representative of modern amphibians.

In this study, we characterized the MHC I in two species of Korean anurans. We estimated MHC IA loci number both in aquatic tadpoles and terrestrial adult life stages. In addition, we characterized allelic genetic diversity and tested for sites under selection. We also constructed phylogenetic trees of amphibians based on their MHC IA sequences and compared these to those based on neutral markers. Finally, we examined the supertype distribution of the alleles and their physiochemical properties that may confer pathogen resistance.

2. Materials and methods

2.1. Animals

We collected six mating pairs of the Asiatic toad, *Bufo gargarizans*, from Geumsan (35°47.073′N, 127°08.490′E) and Jeonju (36°08.256′N, 127°22.891′E), South Korea, and reared their tadpoles in our laboratory. Fifteen metamorphs were used in the experiment. We collected 13 adult Japanese tree frogs, *Hyla japonica*, from four different localities: Chuncheon (37°58.673′N, 127°38.318′E), Gwanak district in Seoul (37°27.48′N, 126°56.50′E), Jirisan National Park, Namwon (35°23.228′N, 127°27.347′E), and Gurye, Jeollanam-do (35°20.139′N, 127°27.290′E). We also collected a mating pair of *H. japonica* from Cheongbuik-Myeon, Gyeonggi-do (37°02.383′N, 126°52.789′E) to obtain tadpoles.

Thirty tadpoles of each species were raised in 40 L tanks until stages 27–37 (Gosner, 1960). Larvae were fed a plant-based (curled mallow) diet supplemented with fish food protein tablets. Five *B. gargarizans* and two *H. japonica* tadpoles in mid- and early-toe differentiation and developmental stages (Table S7) were used to test for the presence of MHC IA transcripts in tadpoles.

All experimental protocols were approved by Seoul National University Institutional Animal Care and Use Committee (IACUC), permit number SNU-150330-5.

2.2. Nucleic acid extraction

All tadpoles used in the experiment were euthanized in tricaine methanesulfonate, MS-222 (Torreilles et al., 2009), and tissues immediately excised for RNA extraction. Livers were dissected from adults. For tadpoles and metamorphs, the livers were dissected with surrounding tissues. RNA was extracted from tissues using RNeasy Micro and Mini kits (Qiagen, Valencia, CA, USA), following the manufacturer's instructions.

2.3. Amplification of MHC IA

Rapid amplification of cDNA ends (RACE) PCR can be used to obtain full length cDNAs when only a short stretch of sequence within the mRNA is known (Scotto-Lavino et al., 2006). Therefore, to amplify the complete peptide region (PBR) that spans exons 2 and 3, the 5′ RACE protocol was followed as described by Scotto-Lavino et al. (2006).

2.3.1. cDNA and RACE primer design

Total RNA (1 μg) extracted from the livers of three *H. japonica* adults was used to synthesize cDNA using the PrimeScript First Strand cDNA Synthesis kit (Takara, Otsu, Shiga, Japan) according to the manufacturer's instructions. To amplify classical MHC I loci in *H. japonica*, published MHC IA sequences from *Espadarana prosoblepon* (accession numbers: JQ679332 – JQ679341) and *Smilisca phaeota* (accession numbers: JQ679380 – JQ679390) were aligned using Geneious v7.1.4 (Kearse et al., 2012). Forward and reverse primers were designed in conserved regions to amplify a region spanning the final 143 base pairs (bp) of exon 3 to the first 178 bp of exon 4. These primers, ESSM F1 and ESSM R1 (see Table S2 for all primer sequences) amplified a 319 bp fragment using the following cycling parameters in an Applied Biosystems (Foster City, CA, USA) Veriti 96-Well Thermal Cycler: 95 °C for 2 min, 30 cycles of 94 °C for 20 s, 55 °C for 30 s, and 72 °C for 45 s, and a final elongation step of 72 °C for 3 min.

The fragments were cloned, and ten colonies from each transformation were amplified using whole colony PCR with M13 primers and the following PCR conditions: 95 °C for 2 min, 30 cycles of 94 °C for 20 s, 55 °C for 20 s, 72 °C for 1 min, and a final elongation step of 72 °C for 3 min. The amplicons were prepared for sequencing using a standard exonuclease/phosphatase treatment and Sanger sequenced (Macrogen, Seoul, Korea). When aligned, the fragments were highly polymorphic and a BLAST search of each fragment showed homology to known anuran MHC IA sequences, indicating that the primer set successfully amplified MHC IA loci in *H. japonica*. Next, using the *H. japonica* MHC IA alignment, three additional 5' RACE primers, internal to ESSM R1, were designed in conserved regions of exon 4. These gene specific primers were named GSP-1 (= ESSM R1), GSP-2, and GSP-3 (Table S2).

2.3.2. 5' RACE

Reverse transcriptase (Takara) and the primer GSP-1 were used to synthesize cDNA from three different RNA extracts of *H. japonica* liver tissue. The cDNA was purified (Gel/PCR purification kit, Favorgen Biotech, Pintung, Taiwan), and a poly(A) tail was ligated to the 3′ hydroxyl terminus of the cDNA fragments using the following reaction: 20 μl of purified non-diluted cDNA dilution, 3.5 μl of 10 × terminal transferase reaction buffer, 4 μl dATP, 5 μl 2.5 mM $CoCl_2$, and 0.5 μl terminal transferase (New England Biolabs, Ipswich, MA, USA), which were combined and incubated at 37 °C for 10 min, 65 °C for 5 min, and ice for 2 min. The sample then was diluted with H_2O to a final volume of 500 μl.

MHC IA fragments were amplified from this dilution of A-tailed cDNA in two amplification rounds. To increase the likelihood of amplifying MHC IA, two gene-specific primers were used in two separate first rounds of amplification, with the resulting PCR products subsequently used for corresponding separate second rounds of amplification. In the first round of amplification, a gene-specific primer, GSP-1 or GSP-2, a hybrid primer that contains a unique 35- base oligonucleotide sequence and a poly-T sequence (Table S2), Q_t, and Q_o were used in the following PCR: 98 °C for 5 min, 48 °C for 2 min, 72 °C for 40 min, 30 cycles of 94 °C for 10 s, 55 °C for 10 s, 72 °C for 3 min, and a final elongation step at 72 °C for 12 min, run in a Veriti 96-Well Thermal Cycler (Applied Biosystems). Next, a nested PCR was performed using a 1:20 dilution of the amplicons (from both GSP-1 and GSP-2) and the internal primers GSP-3 and Q_i. PCR conditions were as follows: 95 °C for 3 min, 30 cycles of 94 °C for 10 s, 55 °C for 10 s, 72 °C for 3 min, and a final elongation step at 72 °C for 12 min. The PCR product (1 μl) was run on a 1.5% agarose gel to confirm the amplification. Bands were excised from the gel, purified, and cloned using the methods described above.

Five colonies from each transformation were prepared for Sanger sequencing using the methods described above. BLAST results of these sequences confirmed that the 5' RACE amplified an 813 bp fragment of MHC IA spanning 96 bp of exon 1 to 177 bp of

exon 4. From these sequences, a forward primer (X1F1) was designed in the conserved region of exon 1 and used in conjunction with GSP-1 to amplify a 744 bp fragment of MHC IA in *H. japonica* (Table S2). This primer set also amplified a 741 bp MHC IA fragment in cDNA synthesized from RNA isolated from liver tissue of *B. gargarizans* juveniles.

2.4. MHC IA genotyping

Total RNA (1 μg) and 0.5 μl Q_t were brought to a final volume of 11.75 μl with H_2O and heated to 80 °C for 1 min to disrupt secondary structure and allow primer binding. This then was combined with a master mix of: 4 μl 5 × reverse transcription buffer, 1 μl 10 mM dNTP, 2 μl 0.1 M DTT (dithiothreitol), 0.25 μl (10 U) RNasin, and 1 μl (200 U) RTase. cDNA was synthesized using the following PCR parameters: 42 °C for 60 min, 50 °C for 10 min, and 70 °C for 15 min. The RNA template was destroyed with an RNase treatment at 37 °C for 20 min. The cDNA template was diluted 1:10 for use in PCR with X1F1 and GSP-1, and the following PCR conditions were used: 95 °C for 2 min, 30 cycles of 94 °C for 20 s, 55 °C for 30 s, 72 °C for 45 s, and a final elongation step of 72 °C for 3 min.

For two individuals of each species, independent PCRs were run to test samples in duplicate. Since the primers were designed in highly conserved regions, only one band was visualized on gels. PCR products were purified, ligated, and cloned using a RBC T&A cloning vector kit (RBC Bioscience, Taipai, Taiwan) and DH5α competent *Escherichia coli* cells (Real Biotech, Taipei, Taiwan). Cells were grown on LB agar plates for 16–18 h at 37 °C, and blue-white screening was used to select colonies with positive transformants from each individual. An average of 21 clones per sample was Sanger sequenced on an Applied Biosystems 3730xl DNA Analyzer (Macrogen, Seoul, Korea).

2.5. Sequence alignment and variant verification

After trimming the vector and primer sequences, a 744 bp MHC IA sequence was isolated in *H. japonica* and a 741 bp sequence in *B. gargarizans*. Sequences were translated and any containing stop codons or indels were removed. A cloned sequence was accepted as a valid allele only if it was isolated in independent PCRs (from two individuals or from two reactions from the same individual). BLAST (NCBI; Altschul et al., 1990) was used to confirm homology of sequences to MHC IA in other anuran species. The sequences spanned 27 bp of exon 1, the full length of exon 2 (261 bp) and exon 3 (279 bp) (exons 2 and 3 encode the entire peptide binding region), and 174–177 bp of exon 4. The difference in MHC IA sequence lengths between the two species is attributable to the presence of an amino acid in exon 4 of *H. japonica* that was absent in *B. gargarizans*.

To prevent false allele classification resulting from sequencing errors, alleles were considered likely to be the same if they varied by 4 bp or less. However, if identical variants were identified in multiple PCRs and cloning rounds, these variants were treated as authentic irrespective of the number of bp substitutions. To denote similarity, these variants were numbered as #.5 (e.g., a sequence similar to putative allele 8 was numbered 8.5).

2.6. Data analyses

2.6.1. Genetic diversity

The validated variants were translated and aligned to *Xenopus laevis* (accession number: AF185579) and human luekocyte antigen (HLA)-A (accession number: AJ621243) to predict exon boundaries. Sequences then were partitioned into exons and analyzed separately using DnaSP v5.10 to compute species-specific polymorphic sites (segregating, S), nucleotide differences (k), and nucleotide diversity (π). MEGA v6.06 (Tamura et al., 2013) was used to calculate average pairwise nucleotide distance (Kimura-2 parameter) and Poisson-corrected amino acid distances with 500 bootstrap replicates.

2.6.2. Selection and recombination

For both species, an alignment of validated variants was generated and antigen binding sites (ABS) were identified using the ABS of *X. laevis* (Flajnik et al., 1991, 1999), denoted as *Xela* ABS. However, as these same codon positions have not been shown to be common to all amphibians, a Wu-Kabat analysis also was conducted. Briefly, variability is calculated by dividing the number of amino acids at a position by the frequency of the most common amino acid, thereby predicting amino acids likely subject to selection (Wu and Kabat, 1970). A site was identified as likely to be under selection if the Wu-Kabat variability metric was greater than twice the average of Wu-Kabat values for all sites, and such sites were denoted W-K (Wu-Kabat).

To identify amino acids under positive selection, the HyPhy package was implemented on the molecular evolution analysis platform Datamonkey (Delport et al., 2010; Kosakovsky Pond and Frost, 2005). First, genetic algorithm recombination detection (GARD) was employed to locate non-recombinant fragments and construct phylogenetic trees for respective partitions (Kosakovsky Pond et al., 2006). To prevent models from erroneously identifying selected sites owing to the presence of recombinant sequences, these GARD-inferred trees were used to implement three likelihood models: random-effects likelihood (REL), fixed-effects likelihood (FEL), and mixed-effects model of evolution (MEME). The REL model uses Bayes factors (BF) to infer sites under selection (Kosakovsky Pond and Frost, 2005). Since REL uses the entire alignment to make inferences about rates at each site, it can detect the most sites but is also prone to identify the most false positives (Poon et al., 2009). Thus, the likelihood methods FEL and MEME, which can identify instances of both episodic and positive selection (Murrell et al., 2012), also were run.

To avoid incorporating false positives, a conservative method was adopted whereby only sites that were indicated by at least two methods ($p < 0.05$, BF > 100) were retained as positively selected sites (PSS). Alleles were partitioned (Table S3), and all subsequent tests were conducted on species-specific alignments, except when a combined alignment was possible (i.e., when identified sites were identical, such as *Xela* ABS). A modified Nei-Gojobori (Jukes-Cantor) model was used to conduct a codon-based Z-test for selection with 500 bootstrap replicates in MEGA v6.06 (Jukes and Cantor, 1969; Nei and Gojobori, 1986; Tamura et al., 2013). Synonymous Non-synonymous Analysis program (SNAP) v2.1.1 also was used to calculate d_N, d_S, and d_N/d_S (www.hiv.lanl.gov), with $d_N/d_S > 1$ indicative of positive selection and $d_N/d_S = 1$ of neutral evolution.

2.6.3. Phylogenetic trees

Available anuran MHC IA sequences were downloaded from NCBI and aligned with the generated *B. gargarizans* and *H. japonica* allelic libraries. The entire alignment of 193 amphibian sequences from a total of 16 species (Fig. 1) was then used to construct a neighbor-joining (NJ) tree in MEGA v6.06. Owing to variation in the amount of sequence information in exon 2 over this wide range of species, the alignment was trimmed to include only exon 3 and exon 4 through the endpoint of *B. gargarizans* and *H. japonica* sequences. *Xenopus laevis* sequences were included and the salamander *Ambystoma mexicanum* served as an outgroup. The modified Nei-Gojobori (Jukes-Cantor correction) model was used and only synonymous sites were considered, with pairwise deletion and 500 bootstrap replicates. To verify the identity of sequences (e.g., classical IA vs. non-classical IB loci), we also

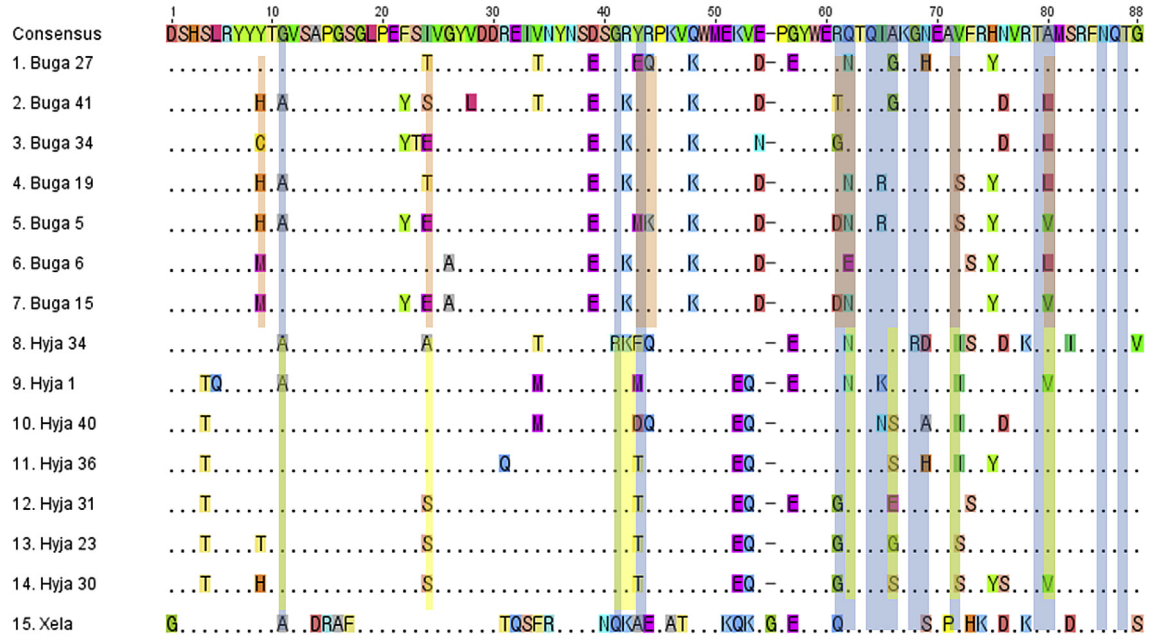

Fig. 1. MHC IA alpha 1 domain amino acid alignment. Buga = *Bufo gargarizans*, Hyja = *Hyla japonica*, Xela = *X. laevis*, accession code: AF185579 *Xela* antigen binding sites (ABS) are highlighted in blue, *B. gargarizans* positively selected sites (PSS) in orange, and *H. japonica* PSS in yellow. Amino acid alignments for alpha 1 and 2 domains are shown in Figure S1. (For interpretation of the references to color in this figure legend, the reader is referred to the web version of this article.)

generated a NJ tree of known anuran MHC IA and IB sequences using a Poisson model with pairwise deletion and 500 bootstrap replicates.

Recombination in anurans has been found to occur around exon boundaries (Bos and Waldman, 2006; Zhao et al., 2013), and substitution rates were found to differ in exons 2 and 3 of the peptide binding region (PBR) and exon 4 of the non-PBR. Therefore, all exons were analyzed separately for subsequent maximum likelihood (ML) and Bayesian analyses to more accurately reconstruct relationships. Approximately six alleles from each species (unless fewer alleles were available) were retained from the original 193 sequences in each exon dataset: (a) exon 2, (b) exon 3, and (c) exon 4. Positions with gaps were deleted from all alignments.

Maximum likelihood (ML) trees were constructed in MEGA v6.06. Selection of the best-fitting substitution models for each dataset was conducted based on the model with the lowest Bayesian information criterion (BIC) scores, calculated in MEGA v6.06. Hasegawa-Kishino-Yano (HKY85), Tamura-Nei (TN93), and Kimura 2-parameter (K2P) were the best-fitting models for the exon 2, exon 3, and exon 4 datasets, respectively (Hasegawa et al., 1985; Kimura, 1980; Tamura and Nei, 1993). Discrete gamma distribution was implemented on exons 2 and 3, and gamma distribution with invariant sites used for the exon 4 dataset, as indicated by the best-fitting model test in MEGA v6.06. Branch support was calculated using 1000 bootstrap replicates.

Bayesian trees were constructed with the Geneious plug-in MrBayes v3.2.2 for the same three datasets (Huelsenbeck and Ronquist, 2001). The most complex substitution model, general time reversible (GTR), was implemented (Tavaré, 1986). *Xenopus laevis* was set as an outgroup, and gamma rate variation was implemented with four heated chains, a burn-in of 100,000 and a subsampling frequency of 200.

2.6.4. Supertyping

To characterize the functional diversity of MHC IA variants, we conducted a supertyping analysis. The method groups functionally similar alleles together according to the physiochemical properties of individual amino acids, thereby forming clusters of alleles with similar antigen binding motifs (Doytchinova and Flower, 2005). Supertypes were generated by aligning all amino acids sequences and retaining only sites that are involved in peptide binding, specifically those codons contributing to *Xela* ABS. Retained sites were characterized by five physiochemical descriptor variables: z1 (hydrophobicity), z2 (steric bulk), z3 (polarity), and z4 and z5 (electronic effects) and placed into a matrix (Sandberg et al., 1998).

Discriminant analysis of principle components (DAPC) was used to describe functional clusters in the adegenet 2.0–0 package in R v. 3.2.1 (Jombart, 2008; Jombart et al., 2010). In the analysis, we used K-means clustering with Bayesian information criterion (BIC) to identify the optimal number of clusters. The cross-validation command (xvalDapc) was used to objectively optimize selection of the number of principal components (PCs) to be retained. From this, DAPC assigned alleles to clusters, corresponding to supertypes.

Alleles were sorted by supertype and amino acids that were 100% conserved among all supertypes removed from further analysis. Finally, the frequency of each amino acid was calculated and the z values used to calculate a composite z1 through z5 score for each supertype.

3. Results

3.1. Allele characterization

We characterized the entire MHC IA peptide binding region (PBR) of both *H. japonica* and *B. gargarizans*. The sequenced fragments were 744 bp in *H. japonica* and 741 bp in *B. gargarizans*. *Hyla japonica* had one more amino acid in exon 4 than *B. gargarizans*. These fragments span exons 1 to 4 and encode nine codons of the signal peptide, the entire alpha 1 (87 codons) and alpha 2 (93 codons) domains, and 58–59 codons of the alpha 3 domain. We recovered one to eight unique cDNA sequences per individual, all with high similarity (>80% nucleotide identity) to other anuran MHC IA genes. In total, we isolated 27 putative MHC IA alleles from *B. gargarizans* and 23 from *H. japonica* (Table S4; GenBank accession

numbers: KY302832-KY302858 for *B. gargarizans* and KY302809-KY302831 for *H. japonica*). The putative MHC IA peptides encoded by these alleles demonstrated the highest similarity (computed in Geneious v7.1.4) to the bufonid *Rhinella marina* for *B. gargarizans* and the hylid *Smilisca phaeota* for *H. japonica*.

Compared to *X. laevis* (AF185579), both species had one less amino acid in exon 2, but only *B. gargarizans* had one less amino acid in exon 4 (Fig. 1, S1). Also, *B. gargarizans* and *H. japonica* had four and three less amino acids, respectively, than human leukocyte antigen (HLA) (AJ621243). Many amino acids known to have functional significance, such as sites involved in salt bonds, disulfide bonds, and glycosylation sites (Flajnik et al., 1999; Saper et al., 1991), were evolutionarily conserved across both species.

Although most putative alleles in *H. japonica* appeared to be population-specific, three alleles were expressed by individuals from multiple localities. *Hyja* 8 (*H. japonica* allele 8) was present in two populations (Seoul and Gurye), *Hyja* 18 in three populations (Chuncheon, Seoul, and Gyeonggi-do), and *Hyja* 1 was found in individuals from all five sampling locations. Also, some alleles were more commonly found than others: *Buga* 8.5 and *Hyja* 40 were only expressed in one individual, but *Buga* 2, *Buga* 11, *Buga* 16, *Hyja* 1, *Hyja* 8, and *Hyja* 18 were expressed in five or more individuals (Table S4).

3.2. Number of loci

Using the conservative variant validation criteria described above, *H. japonica* individuals expressed one to seven alleles and *B. gargarizans* one to eight alleles. Therefore, we estimated a minimum of four expressed MHC IA loci exist in each species (Table 1, S5), the most confirmed in any anuran to date (Table 2). Sequences BLASTed to known amphibian MHC IA genes and exhibited the high levels of polymorphism characteristic of classical MHC class IA loci. Notably, we recovered additional sequences in individuals that we were not able to validate because their presence could not be confirmed in multiple clones from separate PCRs (Table S5, S6). All these sequences contained no stop codons and BLASTed to MHC IA, so these possibly are authentic variants. If this is the case, up to 14 alleles were amplified in some individuals, implying a minimum of seven MHC IA loci in each species.

3.3. MHC I transcripts in tadpoles

MHC IA transcripts were present in all tadpoles (*B. gargarizans* N = 5, *H. japonica* N = 2), spanning early to middle stages of tadpole development. We tested a range of Gosner (1960) stages: 27–29 in *H. japonica* and 34–37 in *B. gargarizans* (Table S7). Furthermore, in one *B. gargarizans* tadpole, seven alleles were confirmed, indicating a minimum of four transcribed loci in tadpoles, the same number found in adults (Table S5).

Gosner stage 27, the earliest stage at which MHC IA transcription was tested and confirmed, corresponds to an early stage of hind limb bud development, well before entering the toe differentiation and development stages (stages 31–39).

Table 1
Summary of allele and loci number.

	Bufo gargarizans	*Hyla japonica*
Sample size[a]	20	15
Number of alleles	27	23
Maximum alleles in an individual	8	7
Minimum transcribed loci	4	4

[a] Sample sizes include tadpoles and adults.

3.4. Genetic diversity

As expected, exons 2 and 3, corresponding to the alpha 1 and 2 domains of the PBR, exhibited higher numbers of segregating sites than exons 1 and 4, which are not directly involved in peptide binding (Table 3). The alpha 1 domain had up to ten times the number of segregating sites and three to four times more nucleotide diversity than the alpha 2 domain (Table 3).

The same tests for polymorphism were run on sequences partitioned into positively selected sites (PSS), non-PSS, Wu-Kabat sites (WK), non-W-K, *X. laevis* antigen binding sites (*Xela* ABS), and *Xela* non-ABS. In all cases, sites likely under positive selection (PSS, W-K, *Xela* ABS) exhibited levels of diversity about an order of magnitude higher than those not under positive selection (non-PSS, non-W-K, *Xela* non-ABS). In addition, *H. japonica* had higher levels of diversity than *B. gargarizans* in five of the six partitions (Table 3).

Using the same six partitions, both pairwise nucleotide distances and amino acid distances were again approximately an order of magnitude higher in partitions containing sites under positive selection (Table S8). *Bufo gargarizans* showed lower levels of divergence than *H. japonica* in all partitions except PSS.

3.5. Detection of recombination and selection

GARD detected recombination at two potential breakpoints (nucleotide sites 180 and 502) in *B. gargarizans* and three in *H. japonica* (nucleotide sites 222, 387, and 504). Of the three tests employed with the Datamonkey platform to test for positive selection, REL found the most sites. Using conservative selection criteria, 14 sites displayed positive selection in *B. gargarizans* and 16 in *H. japonica*. In *B. gargarizans*, eight sites were in the alpha 1 domain and five in the alpha 2 domain. For *H. japonica*, eight were in the alpha 1 domain and six in the alpha 2 domain. In addition, one and two sites were found to be under positive selection in the alpha 3 domain of *B. gargarizans* and *H. japonica*, respectively (Tables S9, S10).

In the *B. gargarizans* MHC IA sequences, the Wu-Kabat analysis (Fig. S2, Table S11) identified nine highly variable amino acid positions in the alpha 1 domain and 13 sites in the alpha 2 domain. In *H. japonica* MHC IA, 13, 7, and 2 sites were indicated in alpha 1, 2, and 3 domains. Datamonkey positive selection tests and the Wu-Kabat analysis showed a high degree of overlap between sites, although more similarities were present in the alpha 1 than alpha 2 domains (Tables S12, S13).

Significant overlap was found among the three methods used to identify sites under positive selection, PSS, W-K, and *Xela* ABS (Tables S12, S13). In the alpha 2 domain, the *Xela* ABS was more similar to W-K than PSS. Twenty-five sites were in the *Xela* ABS, compared to 14 PSS and 21 W-K in *B. gargarizans* and 16 PSS and 22 W-K in *H. japonica*. More PSS and W-K were found in *H. japonica* than *B. gargarizans*, and in both species all but one or two sites were in the alpha 1 and 2 domains.

After partitioning sequences into PSS, non-PSS, W-K, non-W-K, *Xela* ABS, and *Xela* non-ABS, we tested for positive selection using SNAP (Table S14). All partitions composed of sites likely under positive selection had $d_N/d_S > 1$, whereas partitions that excluded these sites were not found to be under positive selection. The codon-based Z test of selection in MEGA produced similar results (Table S15). Based on values calculated for exon partitions, exon 3 had the highest $[d_N - d_S]$ value.

3.6. Phylogenetic analyses

To investigate the evolutionary relationships among anuran

Table 2
Number of transcribed MHC IA loci described in anuran species to date.

Family	Species	No. transcribed MHC IA loci	Source
Bufonidae	*Bufo gargarizans*	4	this study
Bufonidae	*Rhinella marina*	1	Lillie et al., 2014
Centrolenidae	*Espadarana prosoblepon*	2	Kiemnec-Tyburczy et al., 2012
Hylidae	*Agalychnis callidryas*	3	Kiemnec-Tyburczy et al., 2012
Hylidae	*Hyla japonica*	4	this study
Hylidae	*Smilisca phaeota*	3	Kiemnec-Tyburczy et al., 2012
Pipidae	*Silurana (Xenopus) tropicalis*	1	Ohta et al., 2006
Pipidae	*Xenopus laevis*	1	Flajnik et al., 1999; Goyos et al., 2011
Ranidae	*Pelophylax nigromaculatus*	1	Gong et al., 2013
Ranidae	*Rana catesbeiana*	3	Kiemnec-Tyburczy et al., 2012
Ranidae	*Rana clamitans*	3	Kiemnec-Tyburczy et al., 2012
Ranidae	*Rana japonica*	3	Lau et al., 2016
Ranidae	*Rana ornativentris*	3	Lau et al., 2016
Ranidae	*Rana tagoi tagoi*	3	Lau et al., 2016
Ranidae	*Rana temporaria*	1	Teacher et al., 2009
Ranidae	*Rana yavapaiensis*	2	Kiemnec-Tyburczy et al., 2012
Rhacophoridae	*Polypedates megacephalus*	2	Zhao et al., 2013
Rhacophoridae	*Rhacophorus omeimontis*	3	Zhao et al., 2013

Table 3
Polymorphism statistics for different partitions of MHC IA alleles.

Partition	*Bufo gargarizans*				*Hyla japonica*			
	sites	S	K	π	sites	S	K	π
Exon 1	27	5	0.895	0.033 ± 0.008	27	4	0.711	0.026 ± 0.007
Exon 2	261	71	21.760	0.083 ± 0.004	261	65	19.316	0.074 ± 0.008
Exon 3	279	61	19.483	0.070 ± 0.004	279	71	19.988	0.072 ± 0.007
Exon 4	174	10	2.434	0.014 ± 0.001	177	26	7.937	0.045 ± 0.004
PSS	42	30	14.557	0.347 ± 0.015	48	35	15.806	0.329 ± 0.015
Non-PSS	699	117	30.015	0.043 ± 0.002	696	131	32.146	0.046 ± 0.005
W-K	66	47	20.720	0.314 ± 0.012	66	51	22.791	0.345 ± 0.017
Non-W-K	674	100	23.852	0.035 ± 0.002	677	112	25.162	0.037 ± 0.005
Xela ABS	75	41	16.052	0.214 ± 0.014	46	46	17.960	0.239 ± 0.015
Xela non-ABS	666	106	28.520	0.043 ± 0.002	120	120	29.992	0.045 ± 0.005

Sites, number of sites (nucleotides) in a partition; S, segregating or polymorphic sites; K, nucleotide differences; π, nucleotide diversity (± SE).

MHC IA, we constructed a neighbor-joining tree on 193 sequences from 16 species, including the caudate *Ambytsoma mexicanum* as an outgroup (Fig. 2). We also used three separate datasets (exons 2, 3, and 4) from which gaps were removed to construct maximum likelihood and Bayesian trees. The topology from the resulting trees exhibited similar trends irrespective of partition or analytical method; thus, only Bayesian trees are shown (Fig. 3, S3, S4).

Overall, MHC I relationships corresponded to accepted anuran phylogenies (Roelants et al., 2007) (Figs. 2 and 3, S3, S4). The Ranidae and Rhacophoridae grouped together in the superfamily Natatanura, and the Hylidae, Centrolenidae, and Bufonidae grouped together to form the superfamily Nobleobatrachia. Both of these superfamilies were supported by posterior probabilities ≥88% in trees generated by each of the datasets (Fig. 3, S3, S4). A NJ tree generated from known anuran IA and IB sequences supported our assumption that the sequences reported here are indeed from classical MHC IA loci. The anuran IB sequences formed a well-supported cluster (100% bootstrap value), while the sequences in this study formed an equally supported clade (100% bootstrap value) with other anuran IA sequences (Fig. S6).

3.7. Supertyping

Six supertypes were found in *B. gargarizans* and *H. japonica* (Fig. 4, Table S16). Alleles were assigned to their respective supertypes with high membership probability (Fig. S5). Of these supertypes, supertypes 1, 2, and 5 were shared among the two species (Table S17). One of these, supertype 2, had only one *H. japonica* allele, but supertypes 1 and 5 contained at least two alleles from each species. In addition, supertype 6 was characterized from a single *B. gargarizans* allele.

Five amino acids were found to be 100% conserved among all six supertypes. After removing these, 20 amino acids remained and the composite z values were calculated for each supertype (Table S18). Hydrophobicity for the consensus sequences varied among supertypes (Fig. 5). Supertype 1 had the highest composite z1 and z2 values (Table 4); thus it was composed of hydrophilic (z1) amino acids with high molecular weight and surface area (z2). Furthermore, only one allele, *Buga* 11, was confirmed in supertype 6. However, this was the most common allele found in *B. gargarizans*, and was found in ten individuals (Table S4). This supertype had the lowest composite z1 value, indicative of lipophilicity.

4. Discussion

A growing body of evidence suggests that, unlike *Xenopus laevis*, many anuran species express multiple MHC IA loci (Gong et al., 2013; Kiemnec-Tyburczy et al., 2012; Kosch et al., 2017; Lau et al., 2016; Zhao et al., 2013). Results obtained from the model species *X. laevis* (Flajnik et al., 1999; Rollins-Smith et al., 1997), with its single MHC IA locus, cannot be generalized across anurans.

4.1. Number of loci and ontogenetic expression

Our findings suggest that *B. gargarizans* and *H. japonica* express more MHC IA loci than demonstrated in previously characterized

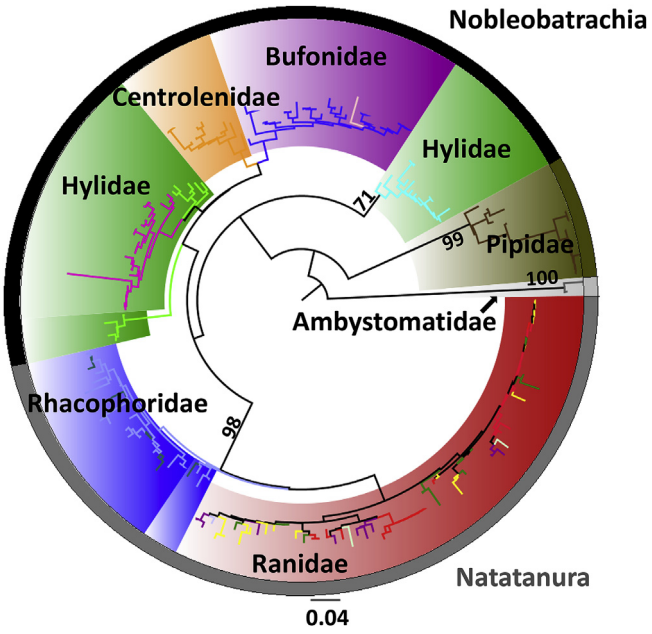

Fig. 2. Evolutionary relationships of amphibian MHC IA. A neighbor-joining tree was constructed in MEGA v6.06 and FigTree v1.4.2 used to make the radial tree. Bootstrap values over 70 are written on the outer branches, and the scale bar represents nucleotide substitutions per site. Families are highlighted and labeled. The Ranidae and Rhacophoridae group together in the superfamily Natatanura (dark gray), and the superfamily Nobleobatrachia (black) is formed by the Hylidae, Centrolenidae, and Bufonidae. Sample names are not shown owing to the large size of the tree, but branch color indicates species. Beginning with *Ambystoma mexicanum* (light gray) and continuing counterclockwise: *Xenopus laevis* (brown), *Agalychnis callidryas*, (turquoise), *Bufo gargarizans* (blue), *Rhinella marina* (light pink), *Espadarana prosoblepon* (orange), *Smilisca phaeota* (lime green), *Hyla japonica* (pink), *Polypedates megacephalus* (dark blue), *Rhacophorus omeimontis* (light blue), *Rana yavapaiensis* (purple), *Pelophylax nigromaculatus* (gray), *Rana clamitans* (yellow), *Rana catesbeiana* (green), *Rana temporaria* (red), and *Rana pipiens* (white). (For interpretation of the references to color in this figure legend, the reader is referred to the web version of this article.)

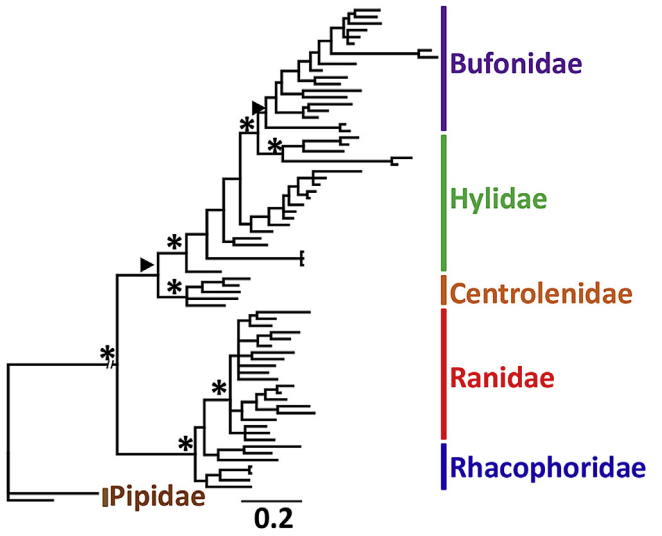

Fig. 3. Exon 2 Bayesian analysis of anuran evolutionary relationships. Alleles in this MHC IA exon 2 (197 bp) tree with *X. laevis* as an outgroup include the following: 2 alleles from the family Pipidae (*X. laevis*; AF185579, AF185582), 20 alleles from the Ranidae (5 alleles from *R. yavapaiensis* [JQ679373, JQ679376 - JQ679379], 6 alleles from *R. clamitans* [JQ679355, JQ679361, JQ679364, JQ679366, JQ679368, JQ679369], 7 alleles from *R. catesbeiana* [JQ679343 - JQ679345, JQ679347, JQ679348, JQ679351, JQ679354], 2 alleles from *R. pipiens* [AF185587, AF185588]), 7 alleles from the Rhacophoridae (3 alleles from *R. omeimontis* [KC261650, KC261651, KC261658] and 4 alleles from *P. megacephalus* [KC261637, KC261639, KC261640, KC261642]); 21 alleles from the Hylidae (6 alleles from *S. phaeota* [JQ679382, JQ679383, JQ679385, JQ679387 - JQ679389], 10 alleles from *H. japonica* [*Hyja* 1, 11, 18, 21, 30, 34, 36, 48, 58, 62 from this study], 5 alleles from *A. callidryas* [JQ679313 - JQ679316, JQ679323]); 19 alleles from the Bufonidae (9 alleles from *B. gargarizans* [*Buga* 2, 4, 11, 16, 19, 27, 34, 35, 41 from this study], 10 alleles from *R. marina* [KC295548, KC295551, KC295553, KC295554, KC295558 - KC295560, KC295566 - KC295568]); 5 alleles from the Centrolenidae (5 alleles from *E. prosoblepon* [JQ679333, JQ679334, JQ679339, JQ679341, JQ679342]). Owing to the large size of the tree, only posterior probabilities on branches corresponding to different families are labeled: * = 0.90–1.0; ▶ = 0.80– 0.89. The scale indicates nucleotide substitutions per site. Families group into superfamilies; the Ranidae and Rhacophoridae form the superfamily Natatanura, and the Hylidae, Centrolenidae, and Bufonidae form the superfamily Nobleobatrachia.

anuran species. Considering only alleles confirmed in independent PCRs, up to seven alleles were expressed in *H. japonica* individuals and eight alleles in *B. gargarizans* individuals. These alleles demonstrate that both species express a minimum of four MHC IA loci, more than the one to three loci described in other anurans (Flajnik et al., 1999; Gong et al., 2013; Kiemnec-Tyburczy et al., 2012; Lau et al., 2016; Lillie et al., 2014; Zhao et al., 2013) (Table 2).

Although all our sequences BLASTed to known MHC IA sequences and exhibited the high levels of polymorphism typical of classical MHC, we cannot exclude the possibility that they represent polymorphic nonclassical MHC class I (MHC IB) sequences. Class IB proteins can be oligomorphic, and numbers of MHC IB genes vary greatly among species (Bahram, 2000; Flajnik et al., 1993). In *X. laevis*, a large number of nonclassical MHC genes have been identified (Edholm et al., 2014; Goyos et al., 2011). However, the sequences in this study only BLASTed to classical genes. Moreover, they show much higher sequence similarity (over 90%) to previously described classical genes than any known nonclassical genes. Additionally, our phylogenetic analysis provides strong evidence that the sequences are from classical MHC IA loci (Fig. S6).

This minimum of four transcribed loci also was confirmed in larvae. Studies in *X. laevis* have failed to find evidence of MHC IA expression, or only subobtimal expression, until larvae approach metamorphosis (Flajnik et al., 1986; Rollins-Smith et al., 1997). Goyos et al. (2009) documented the expression of MHC IB in larvae. Although we have demonstrated the expression of MHC IA transcripts in early larval stages, we have not confirmed the presence of MHC IA proteins. Comparative studies of larval and adult MHC IA expression, using qPCR and protein expression profiles, still are needed, especially in non-model species.

4.2. Phylogenetic analyses

Neighbor-joining, maximum likelihood, and Bayesian trees yielded similar topological trends, forming groupings consistent with anuran phylogenetic trees generated using mitochondrial and nuclear genes (Frost et al., 2006; Roelants et al., 2007). In all trees, the Ranidae and Rhacophoridae group together to form the superfamily Natatanura, while the Hylidae, Centrolenidae, and Bufonidae group together to form the superfamily Nobleobatrachia (Figs. 2 and 3, S3, S4).

In Bayesian trees constructed using exons 2 and 3, the Hylidae appear polyphyletic (Fig. 3, S3) but polyphyly previously has been noted within this family (Darst and Cannatella, 2004; Faivovich et al., 2005; Frost et al., 2006). In the trees based on exon 2 and exon 3, *A. callidryas* forms a polyphyletic group while *H. japonica* and *S. phaeota* group together. In trees based on exon 4 (non-PBR), the Hylidae form a monophyletic group (Fig. S4), in agreement with other studies suggesting that exon 4 of MHC IA more accurately reflects phylogenetic relationships (Nonaka et al., 2011; Zhao et al., 2013). Given the PBR's role in responding to pathogens, variation in exons 2 and 3 may reflect local adaption. Furthermore, the results suggest trans-species polymorphisms, as previously noted in

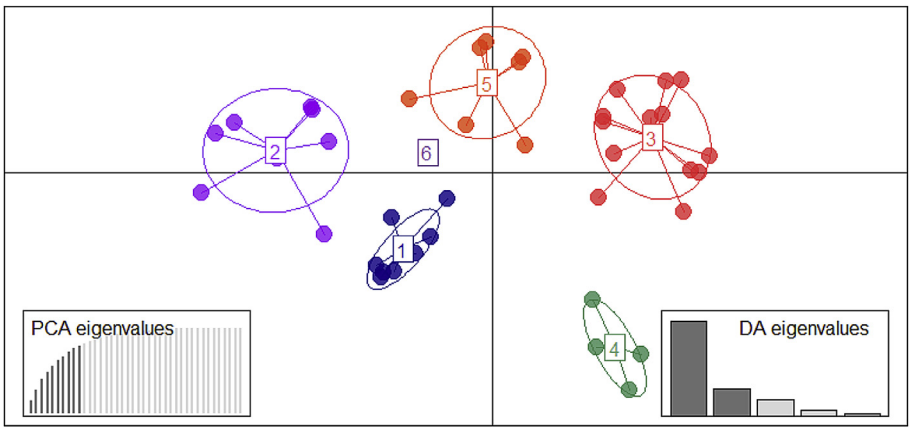

Fig. 4. Supertype scatterplot of *B. gargarizans* and *H. japonica* alleles. Alleles are represented as dots and supertypes as ellipses. Ten principal components (PCs) were retained, as indicated by xvalDapc. The bottom left graph shows the cumulative variance (%) retained by the 10 PCs. The bottom right graph shows eigenvalues retained for the discriminant analysis.

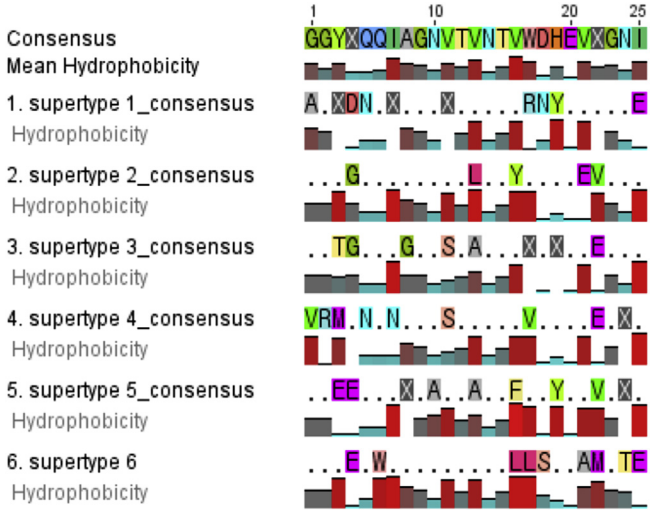

Fig. 5. Hydrophobicity of supertype amino acid motifs. These consensus supertype sequences include the five amino acids that were conserved among all six supertypes. As supertype 6 only had one allele, a consensus was not generated.

studies of anuran MHC IA (Kiemnec-Tyburczy et al., 2012; Lau et al., 2016; Zhao et al., 2013).

4.3. Supertypes and functional properties

The properties of the antigen binding sites determine the binding affinity of encoded MHC molecules; thus, binding motifs are more predictive of antigen binding properties than are individual nucleotide or amino acid differences. Supertyping methodologies facilitate the identification of alleles with similar antigen binding motifs based on their physiochemical properties (Doytchinova and Flower, 2005; Sandberg et al., 1998). Functional properties of the putative MHC IA alleles should reflect their antigen binding and disease resistance properties (Huchard et al., 2008; Schwensow et al., 2007; Sepil et al., 2013).

Of the six total supertypes, three were shared between the two species (Table S17). Based on composite rankings of physiochemical properties, supertype 1, found in both species, exhibits the highest hydrophilicity and steric bulk. Supertype 2 was the only one to be found in all individuals of *B. gargarizans,* but it was only confirmed in *H. japonica* from the Seoul locality.

Supertype 5 has an alanine (A) at the tenth amino acid of the *Xela* ABS, as opposed to the asparagine (N) present in all other supertypes (Fig. 5). Compared to the highly hydrophilic asparagine, alanine is more lipophilic and has less steric bulk (Sandberg et al., 1998). Supertype 5 is shared and was confirmed in over half the *B. gargarizans* individuals and three of the *H. japonica* sampling localities.

Supertype 6 shows the highest lipophilicity and, unlike the other supertypes, contains a tryptophan (W) instead of a glutamine (Q) at the sixth amino acid of the *Xela* ABS (Fig. 5). Tryptophan is highly lipophilic and is the largest amino acid (Sandberg et al., 1998). As supertype 6 includes only *Buga* 11, the allele found in the most *B. gargarizans* individuals (Table S4), this position might be under selective pressure in this species.

Although the species shared three supertypes, some supertypes were unique to either *B. gargarizans* or *H. japonica*. Pathogen communities affecting *B. gargarizans* and *H. japonica* may vary owing to the species' different life history, activity, and behavior: *B. gargarizans* reproduces in lakes, ponds, and small bodies of water in February and March, when temperatures are cold, while *H. japonica* reproduces in streams, small ponds, and rice fields later in the year when temperatures are more moderate. Unique MHC supertypes might facilitate immune responses to particular suites of pathogens.

4.4. Disease resistance and conservation

MHC alleles that confer resistance to pathogens may have important implications for species conservation (Eizaguirre et al.,

Table 4
Supertype hydrophobicity and steric bulk rankings by z1 and z2 composite values.

Z value	Physiochemical properties	Supertype number (composite score)					
z1	Most hydrophilic and polar to lipophilic	S1 (0.541)	S3 (0.361)	S2 (0.244)	S4 (0.241)	S5 (0.120)	S6 (−0.206)
z2	Highest molecular weight and surface area to lowest steric bulk and polarizability	S1 (−0.363)	S4 (−0.376)	S2 (−0.391)	S5 (−0.705)	S6 (−0.947)	S3 (−1.069)

2011; Jäger et al., 2007; Westerdahl et al., 2005). Currently, the unprecedented decline of amphibian populations worldwide is largely attributed to the fungal pathogen *Batrachochytrium dendrobatidis* (Bd). Bd is widely distributed throughout the Korean peninsula, and although both *H. japonica* and *B. gargarizans* show low prevalence of infection, Bd is not known to cause morbidity nor mortality in these species (Bataille et al., 2013). Some Bd strains appear endemic to Asia, and the shared evolutionary history between Bd and Korean anurans may have resulted in the evolution of resistance or tolerance mechanisms within host species, so that contemporary die-offs are not apparent (Bataille et al., 2013; James et al., 2015; Swei et al., 2011). Further studies into geographic patterns of immunogenetic variation corresponding to variation in pathogen loads or strain may clarify how hosts have evolved resistance to Bd.

Although resistance to Bd is associated with particular MHC class II conformations (Bataille et al., 2015), intracellular effects of Bd on physiology and infection dynamics (Berger et al., 2005; Richmond et al., 2009), including interference with lymphocyte-mediated responses to infection (Ellison et al., 2014; Fites et al., 2013), raise the possibility of involvement of MHC class I genes. Moreover, nontraditional pathways of pathogen presentation, such as cross presentation, allow some antigen-presenting cells to present peptides from exogenously derived molecules to MHC I molecules (Cresswell et al., 2005; Neefjes et al., 2011; Vyas et al., 2008).

MHC I also plays a potentially important role in conferring resistance to ranavirus, another important amphibian pathogen (Grayfer et al., 2015; Robert, 2010). MHC IA expression-deficient *Xenopus* tadpoles suffer from higher mortality rates than adults (Gantress et al., 2003; Teacher et al., 2009), demonstrating the importance of class I in conferring resistance to pathogens. Such associations between MHC genotypes and resistance to pathogens recently observed in amphibians highlight the need for a better understanding of the amphibian MHC (Barribeau et al., 2008; Bataille et al., 2015). Further research into the functional properties of immune system genes that confer resistance to pathogens will be facilitated by adopting a supertype approach.

The Bufonidae and Hylidae diverged approximately 70 million years ago (Roelants et al., 2011), yet similarities in their MHC class I sequences imply either convergence or trans-species polymorphism. Selective pressure experienced by species that are exposed to the same or similar pathogens may favor MHC variants with similar binding properties, which might be inferred from their shared MHC IA supertypes.

Data archiving

The MHC IA sequences are available from GenBank, accession numbers: KY302832-KY302858 for *Bufo gargarizans* and KY302809-KY302831 for *Hyla japonica*.

Acknowledgments

We thank Jonathan Fong for advice on the phylogenetic analyses, and David Cannatella, Martin Flajnik, and Neil Gemmell for comments on the manuscript. The research was supported by the National Research Foundation of Korea (2015R1D1A1A01057282) funded by the government of the Republic of Korea (MOE) (to B.W.).

Appendix A. Supplementary data

Supplementary data related to this article can be found at http://dx.doi.org/10.1016/j.dci.2016.12.003.

References

Altschul, S.F., Gish, W., Miller, W., Myers, E.W., Lipman, D.J., 1990. Basic local alignment search tool. J. Mol. Biol. 215, 403–410.
Apanius, V., Penn, D., Slev, P.R., Ruff, L.R., Potts, W.K., 1997. The nature of selection on the major histocompatibility complex. Crit. Rev. Immunol. 17, 179–224.
Babik, W., Pabijan, M., Radwan, J., 2008. Contrasting patterns of variation in MHC loci in the Alpine newt. Mol. Ecol. 17, 2339–2355.
Bahram, S., 2000. MHC genes: from genetics to biology. Adv. Immunol. 76, 1–60.
Barribeau, S.M., Villinger, J., Waldman, B., 2008. Major histocompatibility complex based resistance to a common bacterial pathogen of amphibians. PLoS One 3, e2692.
Bataille, A., Fong, J.J., Cha, M., Wogan, G.O., Baek, H.J., Lee, H., Min, M., Waldman, B., 2013. Genetic evidence for a high diversity and wide distribution of endemic strains of the pathogenic chytrid fungus *Batrachochytrium dendrobatidis* in wild Asian amphibians. Mol. Ecol. 22, 4196–4209.
Bataille, A., Cashins, S.D., Grogan, L., Skerratt, L.F., Hunter, D., McFadden, M., Scheele, B., Brannelly, L.A., Macris, A., Harlow, P.S., Bell, S., Berger, L., Waldman, B., 2015. Susceptibility of amphibians to chytridiomycosis is associated with MHC class II conformation. Proc. R. Soc. B 282, 20143127.
Berger, L., Hyatt, A.D., Speare, R., Longcore, J.E., 2005. Life cycle stages of the amphibian chytrid *Batrachochytrium dendrobatidis*. Dis. Aquat. Organ 68, 51–63.
Bernatchez, L., Landry, C., 2003. MHC studies in nonmodel vertebrates: what have we learned about natural selection in 15 years? J. Evol. Biol. 16, 363–377.
Bjorkman, P.J., Saper, M.A., Samraoui, B., Bennett, W.S., Strominger, J.L., Wiley, D.C., 1987. The foreign antigen binding site and T cell recognition regions of class I histocompatibility antigens. Nature 329, 512–518.
Bonneaud, C., Pérez-Tris, J., Federici, P., Chastel, O., Sorci, G., 2006. Major histocompatibility alleles associated with local resistance to malaria in a passerine. Evolution 60, 383–389.
Bos, D.H., Waldman, B., 2006. Evolution by recombination and transspecies polymorphism in the MHC class I gene of *Xenopus laevis*. Mol. Biol. Evol. 23, 137–143.
Cresswell, P., Ackerman, A.L., Giodini, A., Peaper, D.R., Wearsch, P.A., 2005. Mechanisms of MHC class I-restricted antigen processing and cross-presentation. Immunol. Rev. 207, 145–157.
Darst, C.R., Cannatella, D.C., 2004. Novel relationships among hyloid frogs inferred from 12S and 16S mitochondrial DNA sequences. Mol. Phylogenet. Evol. 31, 462–475.
Delport, W., Poon, A.F., Frost, S.D., Kosakovsky Pond, S.L., 2010. Datamonkey 2010: a suite of phylogenetic analysis tools for evolutionary biology. Bioinformatics 26, 2455–2457.
Doytchinova, I.A., Flower, D.R., 2005. In silico identification of supertypes for class II MHCs. J. Immunol. 174, 7085–7095.
Edholm, E.S., Goyos, A., Taran, J., Andino, F.D.J., Ohta, Y., Robert, J., 2014. Unusual evolutionary conservation and further species-specific adaptations of a large family of nonclassical MHC class Ib genes across different degrees of genome ploidy in the amphibian subfamily Xenopodinae. Immunogenetics 66, 411–426.
Edwards, S.V., Hedrick, P.W., 1998. Evolution and ecology of MHC molecules: from genomics to sexual selection. Trends Ecol. Evol. 13, 305–311.
Eizaguirre, C., Lenz, T.L., Sommerfeld, R.D., Harrod, C., Kalbe, M., Milinski, M., 2011. Parasite diversity, patterns of MHC II variation and olfactory based mate choice in diverging three-spined stickleback ecotypes. Evol. Ecol. 25, 605–622.
Ellison, A.R., Savage, A.E., DiRenzo, G.V., Langhammer, P., Lips, K.R., Zamudio, K.R., 2014. Fighting a losing battle: vigorous immune response countered by pathogen suppression of host defenses in the chytridiomycosis-susceptible frog *Atelopus zeteki*. G3-Genes Genom. Genet. 4, 1275–1289.
Faivovich, J., Haddad, C.F., Garcia, P.C., Frost, D.R., Campbell, J.A., Wheeler, W.C., 2005. Systematic review of the frog family Hylidae, with special reference to Hylinae: phylogenetic analysis and taxonomic revision. Bull. Am. Mus. Nat. Hist. 294, 1–240.
Fellah, J.S., Tuffèry, P., Etchebest, C., Guillet, F., Charlemagne, J., 2002. Cloning and modeling of CD8 β in the amphibian *Ambystoma mexicanum*. Evolutionary conserved structures for interactions with major histocompatibility complex (MHC) class I molecules. Gene 288, 95–102.
Fites, J.S., Ramsey, J.P., Holden, W.M., Collier, S.P., Sutherland, D.M., Reinert, L.K., Gayek, A.S., Dermody, T.S., Aune, T.M., Oswald-Richter, K., Rollins-Smith, L.A., 2013. The invasive chytrid fungus of amphibians paralyzes lymphocyte responses. Science 342, 366–369.
Flajnik, M.F., Du Pasquier, L., 1988. MHC class I antigens as surface markers of adult erythrocytes during the metamorphosis of *Xenopus*. Dev. Biol. 128, 198–206.
Flajnik, M.F., Kaufman, J.F., Hsu, E., Manes, M., Parisot, R., Du Pasquier, L., 1986. Major histocompatibility complex-encoded class I molecules are absent in immunologically competent *Xenopus* before metamorphosis. J. Immunol. 137, 3891–3899.
Flajnik, M.F., Canel, C., Kramer, J., Kasahara, M., 1991. Evolution of the major histocompatibility complex: molecular cloning of major histocompatibility complex class I from the amphibian *Xenopus*. Proc. Natl. Acad. Sci. U. S. A. 88, 537–541.
Flajnik, M.F., Kasahara, M., Shum, B.P., Salter-Cid, L., Taylor, E., Du Pasquier, L., 1993. A novel type of class I gene organization in vertebrates: a large family of non-MHC-linked class I genes is expressed at the RNA level in the amphibian *Xenopus*. EMBO J. 12, 4385–4396.
Flajnik, M.F., Ohta, Y., Greenberg, A.S., Salter-Cid, L., Carrizosa, A., Du Pasquier, L., Kasahara, M., 1999. Two ancient allelic lineages at the single classical class I

locus in the *Xenopus* MHC. J. Immunol. 163, 3826–3833.
Frost, D.R., Grant, T., Faivovich, J., Bain, R.H., Haas, A., Haddad, C.F., De Sá, R.O., Channing, A., Wilkinson, M., Donnellan, S.C., Raxworthy, C.J., Campbell, J.A., Blotto, B.L., Moler, P., Drewes, R.C., Nussbaum, R.A., Lynch, J.D., Green, D.M., Wheeler, W.C., 2006. The amphibian tree of life. Bull. Am. Mus. Nat. Hist. 297, 1–291.
Gantress, J., Maniero, G.D., Cohen, N., Robert, J., 2003. Development and characterization of a model system to study amphibian immune responses to iridoviruses. Virology 311, 254–262.
Gong, J., Sun, Q.P., Xue, F., Fang, S.G., Wan, Q.H., 2013. Molecular characterization of the major histocompatibility complex class Ia gene in the black-spotted frog, *Pelophylax nigromaculata*. Biochem. Genet. 51, 876–888.
Gosner, K.L., 1960. A simplified table for staging anuran embryos and larvae with notes on identification. Herpetologica 16, 183–190.
Goyos, A., Ohta, Y., Guselnikov, S., Robert, J., 2009. Novel nonclassical MHC class Ib genes associated with CD8 T cell development and thymic tumors. Mol. Immunol. 46, 1775–1786.
Goyos, A., Sowa, J., Ohta, Y., Robert, J., 2011. Remarkable conservation of distinct nonclassical MHC class I lineages in divergent amphibian species. J. Immunol. 186, 372–381.
Grayfer, L., Edholm, E.S., Andino, F.D.J., Chinchar, V.G., Robert, J., 2015. Ranavirus host immunity and immune evasion. In: Gray, M.J., Chinchar, V.G. (Eds.), Ranaviruses: Lethal Pathogens of Ectothermic Vertebrates. Springer, Cham, Switzerland, pp. 141–170.
Hasegawa, M., Kishino, H., Yano, T., 1985. Dating of human-ape splitting by a molecular clock of mitochondrial DNA. J. Mol. Evol. 22, 160–174.
Hauswaldt, J.S., Stuckas, H., Pfautsch, S., Tiedemann, R., 2007. Molecular characterization of MHC class II in a nonmodel anuran species, the fire-bellied toad *Bombina bombina*. Immunogenetics 59, 479–491.
Heimeier, D., Baker, C.S., Russell, K., Duignan, P.J., Hutt, A., Stone, G.S., 2009. Confirmed expression of MHC class I and class II genes in the New Zealand endemic Hector's dolphin (*Cephalorhynchus hectori*). Mar. Mam. Sci. 25, 68–90.
Huchard, E., Weill, M., Cowlishaw, G., Raymond, M., Knapp, L.A., 2008. Polymorphism, haplotype composition, and selection in the Mhc-DRB of wild baboons. Immunogenetics 60, 585–598.
Huelsenbeck, J.P., Ronquist, F., 2001. MRBAYES: Bayesian inference of phylogenetic trees. Bioinformatics 17, 754–755.
Hughes, A.L., Yeager, M., 1998. Natural selection at major histocompatibility complex loci of vertebrates. Annu. Rev. Genet. 32, 415–435.
Jäger, I., Eizaguirre, C., Griffiths, S.W., Kalbe, M., Krobbach, C.K., Reusch, T.B.H., Schaschl, H., Milinski, M., 2007. Individual MHC class I and MHC class IIB diversities are associated with male and female reproductive traits in the three-spined stickleback. J. Evol. Biol. 20, 2005–2015.
James, T.Y., Toledo, L.F., Rödder, D., Silva Leite, D., Belasen, A.M., Betancourt-Román, C.M., Jenkinson, T.S., Soto-Azat, C., Lambertini, C., Longo, A.V., Ruggeri, J., Collins, J.P., Burrowes, P.A., Lips, K.R., Zamudio, K.R., Longcore, J.E., 2015. Disentangling host, pathogen, and environmental determinants of a recently emerged wildlife disease: lessons from the first 15 years of amphibian chytridiomycosis research. Ecol. Evol. 5, 4079–4097.
Jombart, T., 2008. adegenet: a R package for the multivariate analysis of genetic markers. Bioinformatics 24, 1403–1405.
Jombart, T., Devillard, S., Balloux, F., 2010. Discriminant analysis of principal components: a new method for the analysis of genetically structured populations. BMC Genet. 11, 94.
Jukes, T.H., Cantor, C.R., 1969. Evolution of protein molecules. In: Munro, R.E. (Ed.), Mammalian Protein Metabolism, vol. 3. Academic Press, New York, pp. 21–132.
Kearse, M., Moir, R., Wilson, A., Stones-Havas, S., Cheung, M., Sturrock, S., Buxton, S., Cooper, A., Markowitz, S., Duran, C., Thierer, T., Ashton, B., Meintjes, P., Drummond, A., 2012. Geneious Basic: an integrated and extendable desktop software platform for the organization and analysis of sequence data. Bioinformatics 28, 1647–1649.
Kiemnec-Tyburczy, K.M., Richmond, J.Q., Savage, A.E., Lips, K.R., Zamudio, K.R., 2012. Genetic diversity of MHC class I loci in six non-model frogs is shaped by positive selection and gene duplication. Heredity 109, 146–155.
Kimura, M., 1980. A simple method for estimating evolutionary rate of base substitutions through comparative studies of nucleotide sequences. J. Mol. Evol. 16, 111–120.
Klein, J., 1986. *Natural History of the Major Histocompatibility Complex*, John Wiley, New York.
Klein, J., Figueroa, F., 1986. Evolution of the major histocompatibility complex. Crit. Rev. Immunol. 6, 295–386.
Klein, J., Sato, A., Nikolaidis, N., 2007. MHC, TSP, and the origin of species: from immunogenetics to evolutionary genetics. Annu. Rev. Genet. 41, 281–304.
Kosakovsky Pond, S.L., Frost, S.D., 2005. Datamonkey: rapid detection of selective pressure on individual sites of codon alignments. Bioinformatics 21, 2531–2533.
Kosakovsky Pond, S.L., Posada, D., Gravenor, M.B., Woelk, C.H., Frost, S.D., 2006. GARD: a genetic algorithm for recombination detection. Bioinformatics 22, 3096–3098.
Kosch, T.A., Eimes, J.A., Didinger, C., Brannelly, L.A., Waldman, B., Berger, L., Skerratt, L.F., 2017. Characterization of MHC class IA in the endangered southern corroboree frog. Immunogenetics (in press).
Lau, Q., Igawa, T., Komaki, S., Satta, Y., 2016. Characterisation of major histocompatibility complex class I genes in Japanese Ranidae frogs. Immunogenetics 68, 797–806.
Lillie, M., Shine, R., Belov, K., 2014. Characterisation of major histocompatibility complex class I in the Australian cane toad, *Rhinella marina*. PLoS One 8, e102824.
Loker, E., Hofkin, B., 2015. *Parasitology: a Conceptual Approach*, Garland Science, New York.
Milinski, M., 2006. The major histocompatibility complex, sexual selection, and mate choice. Annu. Rev. Ecol. Evol. Syst. 17, 159–186.
Murrell, B., Wertheim, J.O., Moola, S., Weighill, T., Scheffler, K., Kosakovsky Pond, S.L., 2012. Detecting individual sites subject to episodic diversifying selection. PLoS Genet. 8, e1002764.
Neefjes, J., Jongsma, M.L., Paul, P., Bakke, O., 2011. Towards a systems understanding of MHC class I and MHC class II antigen presentation. Nat. Rev. Immunol. 11, 823–836.
Nei, M., Gojobori, T., 1986. Simple methods for estimating the numbers of synonymous and nonsynonymous nucleotide substitutions. Mol. Biol. Evol. 3, 418–426.
Nonaka, M.I., Aizawa, K., Mitani, H., Bannai, H.P., Nonaka, M., 2011. Retained orthologous relationships of the MHC class I genes during euteleost evolution. Mol. Biol. Evol. 28, 3099–3112.
Ohta, Y., Goetz, W., Hossain, M.Z., Nonaka, M., Flajnik, M.F., 2006. Ancestral organization of the MHC revealed in the amphibian *Xenopus*. J. Immunol. 176, 3674–3685.
Piertney, S.B., Oliver, M.K., 2006. The evolutionary ecology of the major histocompatibility complex. Heredity 96, 7–21.
Poon, A.F., Frost, S.D., Kosakovsky Pond, S.L., 2009. Detecting Signatures of Selection from DNA Sequences Using Datamonkey. In: Posada, D. (Ed.), Bioinformatics for DNA Sequence Analysis. Humana Press, New York, pp. 163–183.
Rammensee, H.G., Bachmann, J., Stevanovic S., 2013. *MHC Ligands and Peptide Motifs*, Springer, Berlin.
Reusch, T.B., Häberli, M.A., Aeschlimann, P.B., Milinski, M., 2001. Female sticklebacks count alleles in a strategy of sexual selection explaining MHC polymorphism. Nature 414, 300–302.
Richmond, J.Q., Savage, A.E., Zamudio, K.R., Rosenblum, E.B., 2009. Toward immunogenetic studies of amphibian chytridiomycosis: linking innate and acquired immunity. Bioscience 59, 311–320.
Robert, J., 2010. Emerging ranaviral infectious diseases and amphibian decline. Diversity 2, 314–330.
Robert, J., Ohta, Y., 2009. Comparative and developmental study of the immune system in *Xenopus*. Dev. Dynam 238, 1249–1270.
Roelants, K., Gower, D.J., Wilkinson, M., Loader, S.P., Biju, S.D., Guillaume, K., Moriau, L., Bossuyt, F., 2007. Global patterns of diversification in the history of modern amphibians. Proc. Natl. Acad. Sci. U. S. A. 104, 887–892.
Roelants, K., Haas, A., Bossuyt, F., 2011. Anuran radiations and the evolution of tadpole morphospace. Proc. Natl. Acad. Sci. U. S. A. 108, 8731–8736.
Rollins-Smith, L.A., 1998. Metamorphosis and the amphibian immune system. Immunol. Rev. 166, 221–230.
Rollins-Smith, L.A., Flajnik, M.F., Blair, P.J., Davis, A., Green, W.F., 1997. Involvement of thyroid hormones in the expression of MHC class I antigens during ontogeny in *Xenopus*. J. Immunol. Res. 5, 133–144.
Salter-Cid, L., Nonaka, M., Flajnik, M.F., 1998. Expression of MHC class Ia and class Ib during ontogeny: high expression in epithelia and coregulation of class Ia and Imp7 genes. J. Immunol. 160, 2853–2861.
Sammut, B., Laurens, V., Tournefier, A., 1997. Isolation of Mhc class I cDNAs from the axolotl *Ambystoma mexicanum*. Immunogenetics 45, 285–294.
Sammut, B., Du Pasquier, L., Ducoroy, P., Laurens, V., Marcuz, A., Tournefier, A., 1999. Axolotl MHC architecture and polymorphism. Eur. J. Immunol. 29, 2897–2907.
Sandberg, M., Eriksson, L., Jonsson, J., Sjöström, M., Wold, S., 1998. New chemical descriptors relevant for the design of biologically active peptides. A multivariate characterization of 87 amino acids. J. Med. Chem. 41, 2481–2491.
Saper, M.A., Bjorkman, P., Wiley, D.C., 1991. Refined structure of the human histocompatibility antigen HLA-A2 at 2.6 Å resolution. J. Mol. Biol. 219, 277–319.
Schwensow, N., Fietz, J., Dausmann, K.H., Sommer, S., 2007. Neutral versus adaptive genetic variation in parasite resistance: importance of major histocompatibility complex supertypes in a free-ranging primate. Heredity 99, 265–277.
Scotto–Lavino, E., Du, G., Frohman, M.A., 2006. 5′ end cDNA amplification using classic RACE. Nat. Protoc. 1, 2555–2562.
Sepil, I., Moghadam, H.K., Huchard, E., Sheldon, B.C., 2012. Characterization and 454 pyrosequencing of Major Histocompatibility Complex class I genes in the great tit reveal complexity in a passerine system. BMC Evol. Biol. 12, 68.
Sepil, I., Lachish, S., Hinks, A.E., Sheldon, B.C., 2013. Mhc supertypes confer both qualitative and quantitative resistance to avian malaria infections in a wild bird population. Proc. R. Soc. B 280, 20130134.
Shum, B.P., Avila, D., Du Pasquier, L., Kasahara, M., Flajnik, M.F., 1993. Isolation of a classical MHC class I cDNA from an amphibian. Evidence for only one class I locus in the *Xenopus* MHC. J. Immunol. 151, 5376–5386.
Swei, A., Rowley, J.J., Rödder, D., Diesmos, M.L., Diesmos, A.C., Briggs, C.J., Brown, R., Cao, T.T., Cheng, T.L., Chong, R.A., Han, B., Hero, J.M., Hoang, H.D., Kusrini, M.D., Le, D.T.T., McGuire, J.A., Meegaskumbura, M., Min, M.S., Mulcahy, D.G., Neang, T., Phimmachak, S., Rao, D.Q., Reeder, N.M., Schoville, S.D., Sivongxay, N., Srei, N., Stöck, M., Stuart, B.L., Torres, L.S., Tran, D.T.A., Tunstall, T.S., Vieites, D., Vredenburg, V.T., 2011. Is chytridiomycosis an emerging infectious disease in Asia? PLoS One 6, e23179.
Tamura, K., Nei, M., 1993. Estimation of the number of nucleotide substitutions in the control region of mitochondrial DNA in humans and chimpanzees. Mol. Biol. Evol. 10, 512–526.

Tamura, K., Stecher, G., Peterson, D., Filipski, A., Kumar, S., 2013. MEGA6: molecular evolutionary genetics analysis version 6.0. Mol. Biol. Evol. 30, 2725–2729.
Tavaré, S., 1986. Some probabilistic and statistical problems in the analysis of DNA sequences. In: Miura, R.M. (Ed.), Some Mathematical Questions in Biology—DNA Sequence Analysis. American Mathematical Society, Providence, Rhode Island, pp. 57–86.
Teacher, A.G., Garner, T.W., Nichols, R.A., 2009. Evidence for directional selection at a novel major histocompatibility class I marker in wild common frogs (*Rana temporaria*) exposed to a viral pathogen (*Ranavirus*). PLoS One 4, e4616.
Torreilles, S.L., McClure, D.E., Green, S.L., 2009. Evaluation and refinement of euthanasia methods for *Xenopus laevis*. J. Am. Assoc. Lab. Anim. Sci. 48, 512.
Tournefier, A., Laurens, V., Chapusot, C., Ducoroy, P., Padros, M.R., Salvudori, F., Sammut, B., 1998. Structure of MHC class I and class II cDNAs and possible immunodeficiency linked to class II expression in the Mexican axolotl. Immunol. Rev. 166, 259–277.
Těšický, M., Vinkler, M., 2015. Trans-species polymorphism in immune genes: general pattern or MHC-restricted phenomenon? J. Immunol. Res. 2015, 838035.
Vyas, J.M., Van der Veen, A.G., Ploegh, H.L., 2008. The known unknowns of antigen processing and presentation. Nat. Rev. Immunol. 8, 607–618.
Westerdahl, H., Waldenström, J., Hansson, B., Hasselquist, D., von Schantz, T., Bensch, S., 2005. Associations between malaria and MHC genes in a migratory songbird. Proc. R. Soc. B 272, 1511–1518.
Wu, T.T., Kabat, E.A., 1970. An analysis of the sequences of the variable regions of Bence Jones proteins and myeloma light chains and their implications for antibody complementarity. J. Exp. Med. 132, 211–250.
Zhao, M., Wang, Y., Shen, H., Li, C., Chen, C., Luo, Z., Wu, H., 2013. Evolution by selection, recombination, and gene duplication in MHC class I genes of two Rhacophoridae species. BMC Evol. Biol. 13, 113.
Zhu, R., Chen, Z.Y., Wang, J., Liao, X.Y., Gui, J.F., Zhang, Q.Y., 2014. Extensive diversification of MHC in Chinese giant salamanders *Andrias davidianus* (Anda-MHC) reveals novel splice variants. Dev. Comp. Immunol. 42, 311–322.